

Electromagnetic-resonance-ultrasound microscopy with isolated langasite oscillator for measuring local elastic constants of multi-phase solids

Jiayong Tian^{a)}, Hirotsugu Ogi, Toyokazu Tada, and Masahiko Hirao

Graduate School of Engineering Science, Osaka University, Osaka 560-8531, Japan

INTRODUCTION

Recently, ultrasonic-atomic-force microscopy¹ has been developed to evaluate elastic property in nanoscale regions of materials. It uses a flexural vibration of a micro-cantilever generated by a piezoelectric transducer, whose free-end tip taps the specimen surface, while scanning the surface. However, many researches neglected the influence of the attached piezoelectric transducer and the clamping condition at the fixed end, which prevents us from yielding quantitative evaluation of stiffness. Here, we present an alternative acoustic microscopy, *electromagnetic-resonance-ultrasound microscopy* (ERUM), to determine the local stiffness of a material. This measures the resonance-frequency shift of a rectangular-parallelepiped piezoelectric langasite (La₃Ga₅SiO₁₄) crystal. It touches the specimen only through a ball-bearing tip. An electric field from a surrounding solenoid coil excites and detects the vibration of the crystal. Thus, neither electrodes nor mechanical contacts are required for the acoustic coupling. Such noncontact excitation and detection of ultrasonic vibrations eliminate the measurement errors associated with the contacting acoustic excitation and detection. Scanning the object surface with this probe and measuring the frequency shift then provide us with a quantitative mapping of elastic constant.

ELECTROMAGNETIC-RESONANCE-ULTRASOUND MICROSCOPY

An oriented rectangular-parallelepiped langasite crystal stands in a solenoid coil. A spherical bearing of tungsten carbide with radius R is bonded at the center of the bottom surface. With the modal calculation, we use such a resonance mode that shows an antinode at the center of the bottom surface, to which the bearing is attached to provide a contact point with the specimen fixed on an X-Y stage. We apply a biasing force F at the nodal points on the upper surface to increase the sensitivity of resonance-frequency shift and minimize the influence of supports.

Langasite is a trigonal symmetry crystal, whose piezoelectric coefficients are two times larger in magnitude than those of quartz so that the vibration can be excited effectively by a dynamic electric field without contact.² Furthermore, the elastic constants show low temperature-derivatives, of the order of 10^{-6} - 10^{-5} K⁻¹, which assures the stable resonance frequencies.

We apply high-power tone bursts to the solenoid coil to cause the vibration of the probe by the converse piezoelectric effect. The vibration of the probe is then received by the same coil with the piezoelectric effect after the excitation. The received signal is fed to a superheterodyne spectrometer to extract the signal amplitude.³

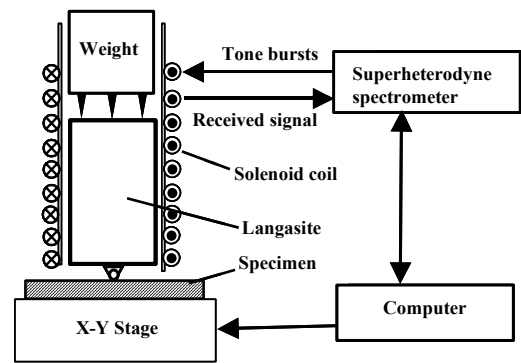


Fig.1 Measurement setup of ERUM

VIBRATION ANALYSIS

To determine the local Young's modulus of the specimen from the resonance frequency of the oscillator, we derive their relationship. We consider the tip-specimen contact as the springs shown in Fig.2. The previous UFAM studies used the simple static Hertz-contact model⁴ to calculate the effective contact stiffness as

$$k_{11}^s = k_{22}^s = 8G^* a, \quad k_{33}^s = \sqrt[3]{6FRE^{*2}}.$$

Here $G^{*-1} = (2 - \nu_1)G_1^{-1} + (2 - \nu_2)G_2^{-1}$, $E^{*-1} = (1 - \nu_1^2)E_1^{-1} + (1 - \nu_2^2)E_2^{-1}$, and $a = \sqrt[3]{3FR/4E^*}$ denotes the contact radius. The subscripts 1 and 2 indicate the bearing and the specimen, respectively. Recently, we showed experimentally and theoretically that this static model failed to explain the contact stiffness because of the complexity of the dynamic contact.^{5,6} Thus, we approximate the effect spring stiffness to be $k_{11} = k_{22} = \alpha k_{11}^s$ and $k_{33} = \beta k_{33}^s$. Here α and β are the dynamic-contact-stiffness factors, which are to be calibrated with reference materials of known elastic constants at a given F .

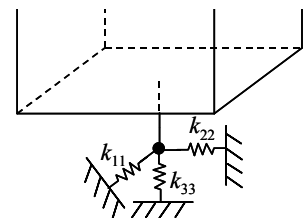


Fig. 2 Contact spring stiffnesses at the tip-specimen interface.

We consider the Lagrangian in a piezoelectric material to calculate the resonance frequencies and vibration modes:

$$\Pi = \frac{1}{2} \iiint_{\Omega} (S_{ij} C_{ijkl} S_{kl} + 2S_{ij} e_{ijk} \phi_{,k} - \phi_{,i} \epsilon_{ij} \phi_{,j} - \rho \omega^2 u_i u_i) dV + \frac{1}{2} \iint_{\Gamma} k_{ij} u_j u_i dS,$$

where S_{ij} , ρ , u_i , and ϕ_i are the strain tensor, mass density, displacement, and electric potential, respectively. Ω and Γ are the volume and the surface of the piezoelectric crystal, respectively. Approximating the displacement and electric potential in terms of linear combinations of the basis functions consisting of normalized Legendre polynomials, stationary point of the Lagrangian provides resonance modes (Rayleigh-Ritz method).

RESULT AND DISCUSSION

Free vibrations of an oriented rectangular parallelepiped of langasite fall into four groups denoted by Ag, Au, Bg and Bu.⁷ Among them, we used the Ag-1 mode because (i) it shows an antinode for the normal displacement u_3 and nodes for the in-plane displacements u_1 and u_2 at the center on the bottom surface, (ii) it shows high sensitivity to the normal contact stiffness k_{33} , (iii) it is easily excited and detected with the solenoid coil and the resonance spectrum shows an ideal lineshape without overlapping any other modes. We can thus neglect the tangential spring stiffnesses k_{11} and k_{22} because of zero in-plane displacements at the contacting point. According to calibration with reference materials,⁶ we calculated the dynamic-contact-stiffness factor to be $\beta \approx 3$.

To illustrate applicability, we obtained Young's-modulus image of a duplex-stainless steel (JIS-SCS13A). The material consists of 25.8%-volume-fraction α (ferrite) phase and 74.2%-volume-fraction γ (austenite) phase: Figure 3 shows the microstructure. The γ -phase particles are precipitated in the α -phase matrix. Figure 4 shows Young's-modulus distribution determined by the measured resonance frequency and the dynamic-contact-stiffness model. It also shows a line trace along the indicated line. Based on the inverse calculation, Young's moduli of the γ phases are $E_{\gamma} = 200$ GPa (brightened part) and 150 GPa (darkened part). We attribute the difference to original grain orientation of the α phase, which dominates the orientation of the γ phase precipitated in it. Young's modulus of α phase is found to be $E_{\alpha} = 121$ -129 GPa, being much smaller than Young's modulus of polycrystalline α -Fe (210.8 GPa). However, large concentration of chromium in α -phase enlarges the lattice parameter and decrease elastic constants as suggested by Tane *et al.*⁸ Indeed, our Young's modulus for the α phase agree with the reported value for a similar duplex-stainless steel.⁸

CONCLUSION

Being based on the vibration of langasite crystal excited by one-point contacting electromagnetic-acoustic-resonance techniques, ERUM shows high potential of measuring the local elasticity of the material. According to the sensitivity and mode analysis, Ag-1 mode is selected for the operating mode of ERUM. We find that the proposed approach is suitable for the ERUM observations and can determine the local elasticity of multiphase and composite materials.

REFERENCES

- ¹Yamanaka, K., and Nakano, S. (1998) Appl. Phys. A, **66**, S313-S317.
- ²Ogi, H., Nakamura, N., Sato, K., Hirao, M., and Uda, S. (2003) IEEE Trans. Ultrason. Freq. Contr., **50**, 553-560.
- ³Fortunko, C. M., Petersen, G. L., Chick, B. B., Renken, M. C., and Preis, A. L. (1992) Rev. Sci. Instrum., **63**, 3477-3486.
- ⁴Johnson, K. L. (1985) *Contact Mechanics* (Cambridge University Press, Cambridge).
- ⁵Tian, J., Ogi, H., Tada, T. and Hirao, M. (2004) J. Acoust. Soc. Am., in press, .
- ⁶Tian, J., Ogi, H., and Hirao, M. J. Appl. Phys., to be published.
- ⁷Mochizuki, E. (1987) J. Phys. Earth, **35**, 159-170.
- ⁸Tane, M., Ichitsubo, T., Ogi, H., and Hirao, M. (2003), Scripta Mater., **48**, 229-234.

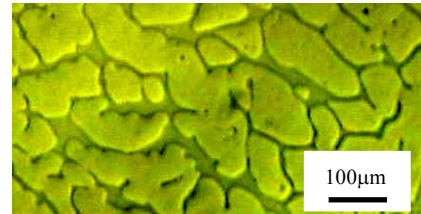


Fig.3 Optical photomicrograph of the duplex stainless steel.

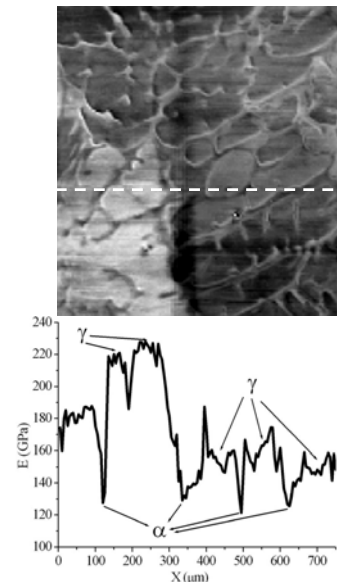


Fig.4 (a) ERUM image of the surface of the duplex stainless steel and (b) line trace of Young's modulus as indicated in (a).